Proc. Natl. Acad. Sci. USA
Vol. 88, pp. 3446–3450, April 1991
Biochemistry

Three-dimensional structure of human basic fibroblast growth factor, a structural homolog of interleukin 1β

(protein crystallography/heparin binding site/receptor recognition)

JIANDONG ZHANG*, LAWRENCE S. COUSENS†, PHILLIP J. BARR†, AND STEPHEN R. SPRANG*‡§

‡Howard Hughes Medical Institute and *Department of Biochemistry, The University of Texas Southwestern Medical Center, 5323 Harry Hines Boulevard, Dallas, TX 75235-9050; and †Chiron Corp., 4560 Horton Street, Emeryville, CA 94608-9910

Communicated by Brian W. Matthews, January 17, 1991

ABSTRACT **The three-dimensional structure of the 146-residue form of human basic fibroblast growth factor (bFGF), expressed as a recombinant protein in yeast, has been determined by x-ray crystallography to a resolution of 1.8 Å. bFGF is composed entirely of β-sheet structure, comprising a three-fold repeat of a four-stranded antiparallel β-meander. The topology of bFGF is identical to that of interleukin 1β, showing that although the two proteins share only 10% sequence identity, bFGF, interleukin 1, and their homologs comprise a family of structurally related mitogenic factors. Analysis of the three-dimensional structure in light of functional studies of bFGF suggests that the receptor binding site and the positively charged heparin binding site correspond to adjacent but separate loci on the β-barrel.**

Basic fibroblast growth factor (bFGF) is the primary inducer of mesoderm formation in embryogenesis, modulating both cell proliferation and differentiation *in vitro* and *in vivo* (1, 2). As a mitogen and chemoattractant, bFGF is a potent mediator of wound repair, angiogenesis, and neural outgrowth. These functions are mediated by interaction with high-affinity cell surface receptors (3, 4) and subsequent alterations in gene expression within responsive cells. Of broad tissue distribution, bFGF induces proliferation and migration of fibroblasts, endothelial cells, and astroglial cells.

bFGF is one of at least seven proteins belonging to the heparin-binding growth factor (HBGF) family (5–7), which includes acidic FGF (aFGF). The two FGFs differ in isoelectric point (bFGF, pI = 9.6; aFGF, pI = 5–6; ref. 5) but share 55% sequence identity and bind to the same receptors (8). At least two oncogenes, *int-2* and *hst/ks* (from stomach tumors and Kaposi sarcoma) are also members of the HBGF family. Multiple forms of active bFGF, generated by amino-terminal proteolysis, have been isolated (9). Here we report the refined three-dimensional structure of recombinant 146-residue bFGF (10).¶ The structure establishes bFGF as a member of the interleukin 1 (IL-1) family and provides a basis for interpretation of functional studies of bFGF with respect to its interaction with high-affinity receptors and with heparin.

Expression and Structure Determination

The synthesis in yeast of an acetylated 154-amino acid human FGF has been described (11). A truncated form, bFGF-(1–146) (10), corresponding to residues 9–154 of the full-length sequence was expressed as an intracellular product in yeast. We chemically synthesized the oligodeoxynucleotides 5′-CATGCCAGCCCTGCCGGAGGMCGGGGGCAGCGG-3′ and 5′-CGCCGCTGCCCCCGTCCTCCGGCAGGGCTGG-3′. These complementary oligonucleotides were ligated to an *Nar* I–*Sal* I fragment encoding amino acids 11–146 of the synthetic hFGF gene (11). The derivatized gene was cloned into the vector pBS100 (12), which contains the alcohol dehydrogenase 2/glyceraldehyde-3-phosphate dehydrogenase (ADH2/GAPDH) hybrid promoter. For expression in yeast, a *Bam*HI–*Sal* I fragment that contained the promoter–gene fusion was cloned into the yeast expression vector pBS24 (13). Yeast cells transformed with pBS24bFGF(1–146) were propagated and induced for expression as described (12, 13) and the recombinant bFGF was purified by heparin-Sepharose chromatography (11).

Crystals of bFGF used for x-ray data collection were grown at room temperature by vapor diffusion. Macroseeded 10-μl sitting drops containing 0.3 mg of bFGF (30 mg/ml), 200 mM sodium succinate (pH 5.3), 60 mM dithiothreitol, and 40% saturated ammonium sulfate were deposited on silanized spot plates and equilibrated in a sealed chamber against a reservoir containing 60% saturated ammonium sulfate in the same buffer. bFGF crystals (space group $P2_12_12_1$, cell constants a = 42.1 Å, b = 86.6 Å, c = 31.9 Å) contain one molecule per asymmetric unit and diffract beyond 1.8-Å resolution.

Diffraction data were measured at room temperature with dual multiwire area detectors of Xuong–Hamlin design (14) with graphite monochromated CuKα x-rays generated by a Rigaku RU-200 rotating-anode source (operating at 50 kV, 108 mA). Data were collected in 0.1° frames about the ω axis of an eulerian goniostat at a rate of 45 sec per frame. Data collection, reduction, merging, and scaling of symmetry-related intensities were accomplished with software by Howard *et al.* (15). Merging statistics are summarized in Table 1.

Experimental crystallographic phases determined by multiple heavy-atom isomorphous replacement (MIR) were based primarily on two derivatives, prepared by soaking crystals in solutions containing $KAu(CN)_2$, which binds to a single site, and EtHgCl, which binds to four sites. Isomorphous and anomalous differences from both of these derivatives were used in phasing. A third derivative, obtained with K_2PtCl_4, was only weakly substituted. All heavy-atom phasing and refinement calculations were performed with the PROTEIN package of computer programs (16). Difference Fourier $|F(\text{native}) - F(\text{derivative})|$ maps, computed with single isomorphous difference phases from the gold derivative, were used to refer all heavy-atom sites to a common origin. The correct hand of the map was chosen by inspection of F(native) electron-density maps computed with both enantiomorphs of the heavy-atom constellation. Heavy-atom refinement statistics are also reported in Table 1. Heavy-atom positions are given in Table 2.

The publication costs of this article were defrayed in part by page charge payment. This article must therefore be hereby marked "*advertisement*" in accordance with 18 U.S.C. §1734 solely to indicate this fact.

Abbreviations: FGF, fibroblast growth factor; aFGF, acidic FGF; bFGF, basic FGF; HBGF, heparin-binding growth factor; IL-1, interleukin 1; MIR, multiple isomorphous replacement.

§To whom reprint requests should be addressed.

¶The atomic coordinates have been deposited in the Protein Data Bank, Chemistry Department, Brookhaven National Laboratory, Upton, NY 11973 (reference 2FGF).

APPENDIX II

SN 08/955,373

Table 1. Data collection and heavy-atom refinement statistics

	Native	EtHgCl	$KAu(CN)_2$	K_2PtCl_4
Soaking conc., mM		2.5	10	1
Soaking time, hr		72	120	12
Resolution, Å	1.8	2.3	2.3	2.9
Measured reflections	46,630	42,074	14,792	20,264
Unique reflections	11,001	9,681	7,818	4,923
R_{merge}	4.56	7.79	5.16	4.27
Completeness	0.974	0.969	0.769	0.999
$\Delta F/F$		0.266	0.323	0.165
R_{Cullis}		0.59	0.71	0.87
F_H/residual		2.14	1.31	0.57

Each data set was collected from a single crystal. The heavy-atom derivatives were refined with their anomalous data. The overall figure of merit was 0.65 to 2.3 Å. The merging R factor is defined as $R_{merge} = [\Sigma_N\Sigma_n(I - \langle I\rangle)/\Sigma_{Nn}\langle I\rangle] \times 100\%$, where N is the number of unique measurements, n is the number of multiple measurements of a particular reflection; I is the measured and $\langle I\rangle$ the mean intensity of a reflection. $\Delta F/F$ is the percent change between native (F_1) and scaled derivative (F_2) data $(\Sigma||F_1| - |F_2||)/\Sigma|F_1|)$. $R_{Cullis} = \Sigma(|F_{der} - F_{ph}|)/\Sigma(|F_{der} - F_{nat}|)$, where F_{nat}, F_{der} and F_{ph} are the native, derivative, and calculated (phased) structure factors, respectively, and the summation is taken over the centric reflections. F_H/residual is the average value of the heavy-atom contribution divided by the lack-of-closure error.

An F_{obs} electron-density map computed at 2.5-Å resolution with figure-of-merit-weighted MIR phases clearly revealed the path of the polypeptide chain comprising residues 18–143 of bFGF (10). An initial model was developed using virtual atoms computed from a ridgeline representation of the electron density by the program BONES (17). An atomic model was obtained by fitting the C^α model to fragments of polypeptide chain derived from a data base of highly refined protein structures, using the DGNL option of FRODO (18).

The model was refined in three cycles (incorporating crystallographic data in the resolution shells 8–2.5 Å, 6–2.0 Å, and 6–1.8 Å) of molecular dynamics-associated crystallographic refinement as implemented in the program X-PLOR (19). After each cycle, the model was refit to a $2F_{obs} - F_{calc}$ map computed with refined phases. A typical X-PLOR cycle consisted of 40 cycles of Powell minimization of stereochemical and x-ray terms, followed by molecular dynamics simulation in which the molecule was allowed to cool slowly from an initial temperature of 2000 K (cycle 1), 1500 K (cycle 2), or 1000 K (cycle 3) to a final temperature of 300 K, using time steps of 0.5 fsec, with 25 K reductions in the temperature of the heat bath every 25 fsec. Restrained refinement of individual atomic temperature factors was carried out after the final cycle.

The model at the present state of refinement comprises 1019 protein atoms corresponding to residues 18–143 (10) and two ordered sulfate ions but no solvent water molecules. The root-mean-square (rms) deviation from ideal covalent bond distances and bond angles is 0.017 Å and 2.9°, respectively, for the refined atomic model. The crystallographic R factor is 0.23 for the data extending from 6.0 Å to 1.8 Å. A volume of the $2F_{obs} - F_{calc}$ electron-density map computed with calculated phases from the present model is shown in Fig. 1. Solvent accessibility calculations were performed using a program written by T. Richmond (Yale University), following the method of Lee and Richards (20).

Structure and Homology to IL-1β

bFGF is composed entirely of antiparallel β-strands, each of which is hydrogen-bonded to β-strands adjacent in the primary sequence. The continuous β-meander forms a barrel

Table 2. Heavy-atom positions

Derivative	Relative occupancy	x	y	z
EtHgCl	4.8	0.3336	0.2314	0.9097
	3.9	0.3605	0.2729	0.0521
	2.3	0.3584	0.2721	0.0128
	0.7	0.2812	0.2388	0.1440
$KAu(CN)_2$	7.6	0.2634	0.2308	0.0536
K_2PtCl_4	2.8	0.3790	0.2058	0.3075
	1.9	0.2898	0.0919	0.3478

closed by the amino- and carboxyl-terminal strands (Fig. 2). The tertiary fold can be decomposed into three copies of a four-stranded β-meander motif, corresponding to residues 18–59 (repeat A), 60–100 (B), and 101–143 (C). The motifs are related by an axis of threefold symmetry, generating a closed barrel. The structural motifs, shown in Fig. 3 *Left*, are remarkably similar to each other, repeats A and B being particularly so.

The first 17 amino-terminal residues of the molecule, rich in serine, glycine, and proline residues (Fig. 4) are not visible in the electron-density map and are apparently disordered. These residues would extend from the "top" of the barrel as depicted in Fig. 2. The carboxyl-terminal 3 residues are also disordered. The core of the bFGF molecule inaccessible to solvent is packed with hydrophobic and aromatic amino acid side chains, while the surface of the molecule is rich in charged amino acids, particularly arginine and lysine, as might be expected from the unusually high pI of the molecule.

The tertiary structure of bFGF is topologically identical to that of IL-1β [refs. 23 and 24; entry 4I1B in the Protein Data Bank (22), submitted by B. Verrapandian, T. L. Poulos, G. L. Gilliland, R. Raag, L. A. Svensson, E. L. Winborne, Y. Masui, and Y. Hirai, April 15, 1990] as expected on the basis of the limited primary sequence similarity of these

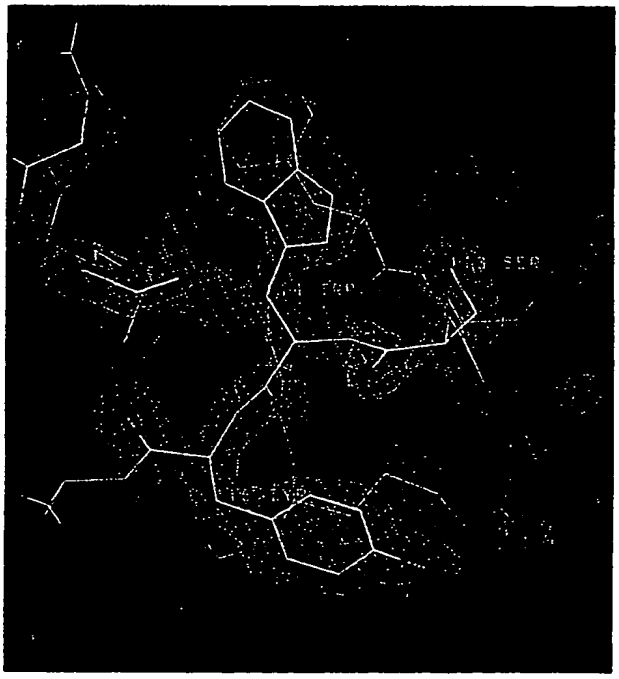

FIG. 1. A volume of the 1.8-Å-resolution $2F_{obs} - F_{calc}$ electron-density map computed with phases derived from the refined coordinates. Ser-113, Trp-114, and Tyr-115 are in the foreground, with Met-76, Arg-107, and Thr-112 in the background. The contour level of the map is 1.65 standard deviations above the mean.

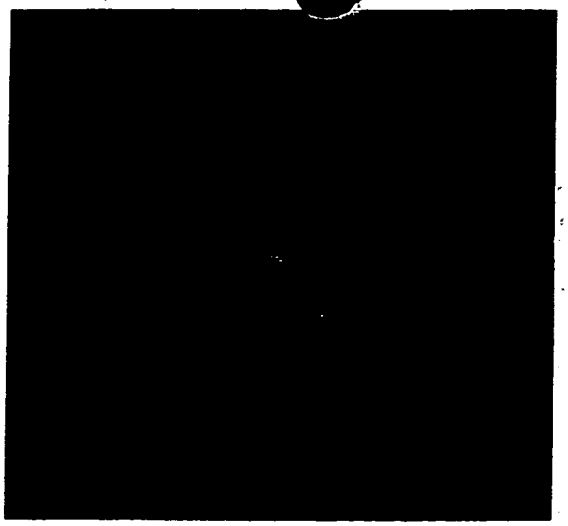

FIG. 2. Ribbon diagram illustrating the tertiary and secondary structure of bFGF. β-Sheet secondary structure is depicted with flattened ribbons. The polypeptide segment (residues 105–115) implicated in receptor recognition is shown in red (see text). The diagram was produced using the computer program RIBBONS by M. Carson (University of Alabama, Birmingham).

proteins (25, 26). The 96 residues comprising the β-cores of bFGF and IL-1β can be superimposed with a rms deviation between corresponding C^{α} positions of 1.55 Å.

The structural superposition, performed both by inspection and automatically using the program O (21), leads to the primary sequence alignment presented in Fig. 4 and allows the definition of "structure conserved sequences" (27, 28). The peptides contained within these sequences adopt similar ϕ and ψ peptide torsion angles and can be superimposed with rms deviations of <1.0 Å. This alignment differs significantly from that of Gimenez-Gallego *et al.* (25).

Favorable structural alignments can also be obtained between IL-1β and circular permutations of the repeat stucture of bFGF. Rotation of bFGF such that repeats CAB are aligned in order with IL-1β ABC gives 109 C^{α} atoms superimposed with rms deviations of 1.98 Å; alignment of bFGF BCA with IL-1β yields 101 C^{α} atoms superimposed with rms deviations of 1.71 Å. However, neither of these alignments generate as many primary sequence matches or as optimal an overlap as does direct superposition.

bFGF contains four cysteine residues, of which two, residues 25 and 92, are conserved in the HBGF family (2). Cys-87 and -92 are positioned on opposite ends of a six-residue turn. None of the four cysteines are involved in disulfide bridges. While the S^{γ} atoms of Cys-87 and -92 are only 7.3 Å apart, the formation of a disulfide bond between them would require a substantial conformational change within the loop. Cys-25 and -69 occupy nearly identical positions in the primary sequence with respect to the underlying topological repeat of the molecule (Fig. 3 *Left*).

bFGF forms oligomers, particularly dimers, under nonreducing conditions. Dimerization possibly occurs between Cys-69 and -87, which are accessible to solvent in the crystal structure and which can be modified by carboxymethylation (29). In contrast, Cys-25 and -92 are totally inaccessible to solvent in the three-dimensional structure. The formation of intermolecular disulfide bridges involving residues 25 and 92 seems unlikely on steric grounds. All four cysteine residues can be replaced by serine residues without loss of biological activity (30, 31), although replacement of Cys-25 and -92 reduces the affinity of bFGF for heparin (30), suggesting that minor structural perturbations may result from the substitution of these buried cysteines.

Location of Potential Receptor and Heparin Binding Sites

Residues 106–115 may form part of the bFGF binding site for the high-affinity receptors (32). These residues form a distorted antiparallel β-turn on the surface of the molecule (Figs.

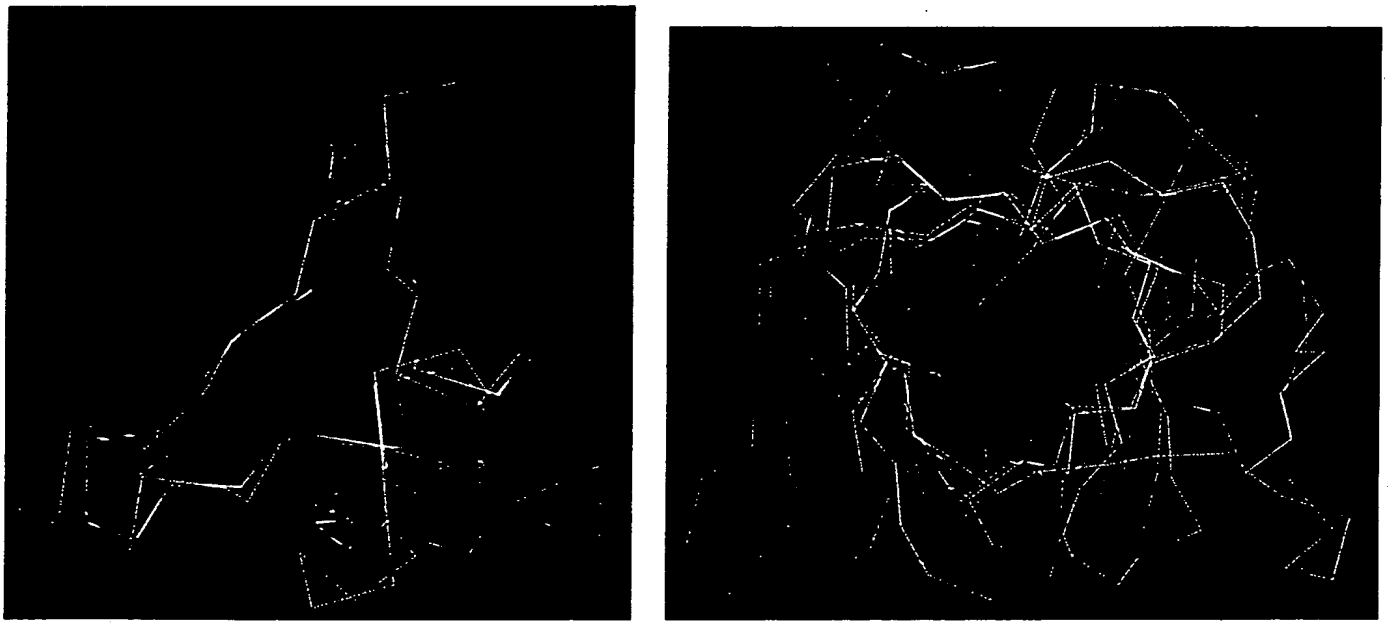

FIG. 3. (*Left*) Superposition of bFGF residues 18–58 in blue (repeat A), 60–100 in red (repeat B), and 101–143 in yellow. Forty-two C^{α} atoms in repeat A can be superimposed onto corresponding positions in repeat B with rms deviation of 1.24 Å; 37 atoms in repeat A can be superimposed with those in repeat C with rms deviation of 1.34 Å. The side-chain atoms of the four cysteine residues in bFGF are shown in green and labeled (SG, for S^{γ}). Superposition calculations were performed using the program O (21). (*Right*) Optimal spatial superposition of the intact C^{α} structures of bFGF (blue) and IL-1β (yellow). The alignment superimposes 96 atoms with rms deviation of 1.55 Å.

```
           20 (7)              40 (26)
            |                   |
bFGF  ....KDPKRLYCKNGGFFLRIHPDGRVDGVREKSDPHI...KLQLQAE
IL1b  APVRSLNCTLRDS.QQKSLVMSGPYELKALHLQGQDMEQQVVFSMSFV
            -------   -----     -----           -----
               *        *

      60 (55)                       80 (78)
       |                            |
bFGF  ER......GVVSIKGVCANRYLAMK..ED.GRLLASKCVT.........D
IL1b  QGEESNDKIPVALGLKEKNLYLSCVLKDDKPTLQLESVDPKNYPKKKMEK
               ------    ------      ------
                *       * **      *   *

              100 (106)           120 (126)
               |                   |
bFGF  ECFFFERLESNNYNTYRSRKYTSWYVALKRTGQYKLGSFTGPGQK.AILF
IL1b  RFVFNKIEI.NNKLEFESAQFPNWYISTSQAENMPVFLGGTKGGQDITDF
      ---------  ------------------                 ----
       .*       **     *     **                 *      *

       143 (150)
         |
bFGF  LPMS
IL1b  TMQFVS
      --
```

FIG. 4. Alignment of the primary sequences of bFGF and human IL-1β (IL-1b). The C^{α} coordinates of IL-1β were obtained from entry 1I1B from the Protein Data Bank (22) and superimposed with corresponding positions in bFGF. The C^{α} positions of corresponding residues shown in boldface are separated by <1 Å on superposition of the polypeptide subsequences in which they are contained. The alignment is identical to that illustrated in Fig. 3 *Right*.

2 and 5). Tyr-114 and Trp-115, implicated as strong binding determinants by peptide competition experiments with synthetic peptides (A. Baird, personal communication), expose 80 $Å^2$ of solvent-accessible surface (20) (versus the ≈260 $Å^2$ expected if the dipeptide were fully exposed). The latter two residues are conserved in the primary sequence of IL-1β. Further, the section of polypeptide chain in which Tyr-114 and Trp-115 are contained forms the longest block of consecutive residues in bFGF that can be superimposed with a corresponding sequence in IL-1β (Fig. 4). FGF and the IL-1 isoforms may thus present similar and corresponding binding surfaces to the extracellular domains of their receptors, both of which belong to the immunoglobulin superfamily (3).

Phosphorylation of bFGF at Thr-112 by protein kinase A increases the affinity of the growth factor for the FGF receptor by a factor of 3–8 (33). The phosphorylation site is contained within the putative receptor binding sequence (Fig. 5). Two nearby arginine residues, 107 and 109, could serve as potential ligands to the phosphothreonine. Modulation of receptor affinity might occur as a direct consequence of electrostatic interactions with Thr(*P*)-112 or as a result of conformational changes induced by phosphorylation. For example, reorientation of Arg-109 to form an ion pair with the phosphothreonine would sever the Arg-109 salt bridge with Glu-57. The activation of glycogen phosphorylase by phosphorylation is triggered by an analogous structural mechanism (34).

Basic and acidic FGF are functionally distinguished by their interaction with heparin. This heterogeneous, sulfated anionic polysaccharide protects both aFGF and bFGF from inactivation by low and high temperature and by acid conditions (35). Heparin potentiates the mitogenic activity of aFGF (5). Removal of 40 amino acids from the amino terminus does not reduce heparin binding. In contrast, deletion of the carboxyl-terminal 40–42 residues of bFGF, a region that is rich in conserved basic residues in both aFGF and bFGF, greatly diminishes heparin affinity (36) but not the ability of bFGF to stimulate DNA synthesis. Reductive methylation of Lys-118 in aFGF (corresponding to Lys-125 in bFGF; ref. 37), or replacement of that residue with glutamate by site-directed mutagenesis (38) substantially decreases the affinity of aFGF for heparin but does not affect its affinity for receptors. These data suggest that the third (C) repeat of FGF contains the heparin binding site.

The binding site for anionic heparin sulfate is likely to be rich in positively charged lysine and arginine residues. However, at least 24 basic residues are exposed on the surface of bFGF. Of those conserved between acidic and basic FGF, 5 residues within the carboxyl-terminal repeat of the molecule (nos. 119, 120, 125, 129, and 135) form a prominent cluster. The quaternary amino groups of Lys-119, -125, and -129 form a nearly equilateral triangle with a mean N^{ζ}–N^{ζ} distance of 8 Å. The two ordered sulfate ions in the crystal structure, one forming ionic contacts with Lys-119 and Lys-129, and the second linking Arg-120 and Lys-125, might mimic heparin sulfate moieties (Fig. 5).

A contour map of the electrostatic potential surface (39) calculated at neutral pH shows a radial and asymmetric distribution of positive charge perpendicular to the pseudo-threefold axis of molecular symmetry (Fig. 6). The most prominent center of positive charge corresponds to the group of conserved lysine and arginine residues described above.

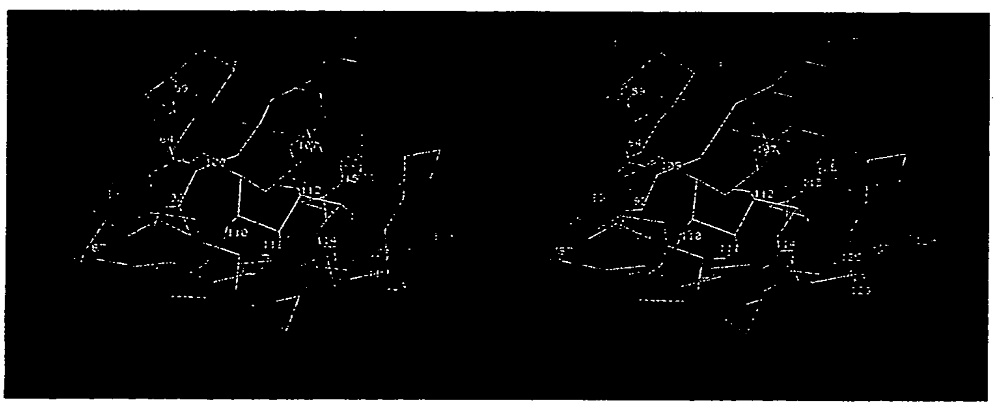

FIG. 5. Side chains of bFGF residues discussed in the text: Glu-59 (ion-pair partner of Arg-109); Ser-64 (protein kinase C phosphorylation site); Arg-107, Arg-109, Lys-110, Tyr-111, Thr-112, Trp-114, and Tyr-115 (putative receptor-binding loop; Thr-112 (protein kinase A phosphorylation site), Lys-119, Arg-120, Lys-125, and Lys-129 (putative heparin binding site). Sulfur atoms of Cys-25, -69, -87, and -93 are shown with van der Waals dot surfaces in yellow. Oxygen atoms are shown in red, nitrogen atoms in magenta, carbon atoms in green, and sulfur in yellow. The C^{α} backbone is colored cyan. Residues 18 and 143 are labeled. Sulfate ions are shown with van der Waals surfaces in cyan.

FIG. 6. Electrostatic potential surface computed using the program DELPHI (38) at the solvent-accessible surface of bFGF. A coulombic boundary condition was used with inner and outer dielectric constants of 2.0 and 80, respectively, an ionic strength of 0.145 M in the solvent region, and a Debye length of 8.0 Å. The negative (red) and positive (blue) potentials are contoured at $2kT$. The ribbon shown in yellow follows the path of the polypeptide chain and the portion of the ribbon in orange (left) marks the position of residues 106–116. The view is perpendicular to the molecular three-fold axis, similar to that shown in Fig. 5.

These are located adjacent to the putative receptor-binding loop (residues 106–115). The apparent spatial separation of the putative heparin and receptor binding sites is consistent with the functional independence of receptor and heparin binding (36, 38) and with the results of inhibition studies with neutralizing antibodies (40).

Most of the residues conserved by aFGF and bFGF are inaccessible to solvent and participate in the stabilization of the hydrophobic core. A conserved but predominantly hydrophobic cluster comprising the carboxyl-terminal triad Phe-139/Leu-140/Pro-141, as well as Tyr-104 and Tyr-24, is exposed to solvent but also appears to serve a structural role, since deletion of the carboxyl-terminal five residues destabilizes and partially inactivates bFGF (36). In general, the sites of sequence identity may be more indicative of structural rather than functional conservation (41).

Note. Two reports of the three-dimensional structure of bFGF have appeared since this manuscript was submitted: an account of the structure of 146-residue bFGF crystallized in space group *P*1 at basic pH [ref. 42 (the paper immediately preceding this one)] and a description of the structures of analogs of acidic and basic FGF (43).

We thank Drs. M. J. Eck and E. Goldsmith for helpful discussions. Two of us (L.S.C. and P.J.B.) thank C. T. Lee Ng for technical assistance and F. Marcus and P. Valenzuela for their support and acknowledge the support of Chiron Corp. and Ethicon, Inc.

1. Whitman, M. & Melton, D. A. (1989) *Annu. Rev. Cell Biol.* **5**, 93–117.
2. Burgess, W. H. & Maciag, T. (1989) *Annu. Rev. Biochem.* **58**, 575–606.
3. Dionne, C. A., Crumley, G., Bellot, F., Kaplow, J. M., Searfoss, G., Ruta, M., Burgess, W. H., Jaye, M. & Schlessinger, J. (1990) *EMBO J.* **9**, 2685–2692.
4. Lee, P. L., Johnson, D. E., Cousens, L. S., Fried, V. A. & Williams, L. T. (1989) *Science* **245**, 57–59.
5. Lobb, R. R., Harper, J. W. & Fett, J. W. (1986) *Anal. Biochem.* **154**, 1–14.
6. Marics, I., Adelaide, J., Raybaud, F., Mattei, M.-G., Coulier, F., Planche, J., de Lapeyriere, O. & Birnbaum, D. (1989) *Oncogene* **4**, 335–340.
7. Finch, P. W., Rubin, J. S., Miki, T., Ron, D. & Aaronson, S. A. (1989) *Science* **245**, 752–755.
8. Neufeld, G. & Gospodarowicz, D. (1986) *J. Biol. Chem.* **261**, 5631–5637.
9. Klagsbrun, M., Smith, S., Sullivan, R., Shing, Y., Davidson, S., Smith, J. A. & Sasse, J. (1987) *Proc. Natl. Acad. Sci. USA* **84**, 1839–1843.
10. Esch, F., Baird, A., Ling, N., Ueno, N., Hill, F., Denoroy, L., Klepper, R., Gospodarowicz, D., Bohlen, P. & Guillemin, R. (1985) *Proc. Natl. Acad. Sci. USA* **82**, 6507–6511.
11. Barr, P. J., Cousens, L. S., Lee-Ng, C. T., Medina-Selby, A., Masiarz, F. R., Hallewell, R. A., Chamberlain, S. H., Bradley, J. D., Lee, D., Steimer, K. S., Poulter, L., Burlingame, A. L., Esch, F. & Baird, A. (1988) *J. Biol. Chem.* **263**, 16471–16478.
12. Barr, P. J., Gibson, H. L., Enea, V., Arnot, D. E., Hollingdale, M. R. & Nussenzweig, V. (1987) *J. Exp. Med.* **165**, 1160–1171.
13. Sabin, E. A., Lee-Ng, C. T., Shuster, J. R. & Barr, P. J. (1989) *Bio/Technology* **7**, 705–709.
14. Hamlin, R., Cork, C., Howard, A., Nielsen, C., Vernon, W., Matthews, D. & Xuong, N.-H. (1981) *J. Appl. Crystallogr.* **14**, 85–93.
15. Howard, A. J., Nielsen, C. & Xuong, N.-H. (1985) *Methods Enzymol.* **114**, 452–472.
16. Steigemann, W. (1989) PROTEIN, A Program System for the Crystal Structure Analysis of Proteins (Max-Planck-Institut für Biochemie, Martinsried, F.R.G.).
17. Jones, T. A. & Thirup, S. (1986) *EMBO J.* **5**, 819–822.
18. Jones, T. A. (1990) *J. Appl. Crystallogr.* **11**, 268–272.
19. Brunger, A. T., Kuriyan, J. & Karplus, M. (1987) *Science* **235**, 458–460.
20. Lee, B. & Richards, F. M. (1971) *J. Mol. Biol.* **55**, 379–400.
21. Jones, T. A., Kjeldgaard, M. (1990) O: Version 5.4 (Univ. of Uppsala, Uppsala).
22. Bernstein, F. C., Koetzle, T. F., Williams, J. B., Meyer, E. F., Jr., Brice, M. D., Rodgers, J. R., Kennard, O., Shimanouchi, T. & Tasumi, M. (1977) *J. Mol. Biol.* **112**, 535–542.
23. Finzel, B. C., Clancy, L. L., Holland, D. R., Muchmore, S. W., Watenpaugh, K. D. & Einspahr, H. M. (1989) *J. Mol. Biol.* **209**, 779–791.
24. Priestle, J. P., Schär, H.-P. & Grütter, M. G. (1989) *Proc. Natl. Acad. Sci. USA* **86**, 9667–9671.
25. Gimenez-Gallego, G., Rodkey, J., Bennett, C., Rios-Candelore, M., DiSalvo, J. & Thomas, K. (1985) *Science* **230**, 1385–1388.
26. Thomas, K. & Gimenez-Gallego, G. (1986) *Trends Biochem. Sci.* **11**, 81–84.
27. Greer, J. (1981) *J. Mol. Biol.* **153**, 1027–1042.
28. Greer, J. (1990) *Proteins* **7**, 317–334.
29. Fox, G. M., Schiffer, S. G., Rhode, M. F., Tsai, L. B., Banks, A. R. & Arakawa, T. (1988) *J. Biol. Chem.* **263**, 18452–18458.
30. Seno, M., Sasada, R., Iwane, M., Sudo, K., Kurokawa, T., Ito, K. & Igarashi, K. (1988) *Biochem. Biophys. Res. Commun.* **151**, 701–708.
31. Arakawa, T., Hsu, Y.-R., Schiffer, S. G., Tsai, L. B., Curless, C. & Fox, G. M. (1989) *Biochem. Biophys. Res. Commun.* **161**, 335–341.
32. Baird, A., Schubert, D., Ling, N. & Guillemin, R. (1988) *Proc. Natl. Acad. Sci. USA* **85**, 2324–2328.
33. Fiege, J.-J. & Baird, A. (1989) *Proc. Natl. Acad. Sci. USA* **86**, 3174–3178.
34. Sprang, S. R., Acharya, K. R., Goldsmith, E. J., Stuart, D. I., Varvill, K., Fletterick, R. J., Madsen, N. B. & Johnson, L. N. (1988) *Nature (London)* **336**, 215–221.
35. Gospodarowicz, D. & Cheng, J. (1986) *J. Cell. Physiol.* **128**, 475–484.
36. Seno, M., Sasada, R., Kurokawa, T. & Igarashi, K. (1990) *Eur. J. Biochem.* **188**, 239–245.
37. Harper, J. W. & Lobb, R. R. (1988) *Biochemistry* **27**, 671–678.
38. Burgess, W. H., Shaheen, A. M., Ravera, M., Jaye, M., Donohue, P. J. & Winkles, J. A. (1990) *J. Cell Biol.* **111**, 2129–2138.
39. Gilson, M., Sharp, K. & Honig, B. (1990) *J. Comp. Chem.* **9**, 327–335.
40. Kurokawa, M., Doctrow, S. R. & Klagsbrun, M. (1989) *J. Biol. Chem.* **264**, 7686–7691.
41. Eck, M. J. & Sprang, S. R. (1989) *J. Biol. Chem.* **264**, 17595–17605.
42. Eriksson, A. E., Cousens, L. S., Weaver, L. H. & Matthews, B. W. (1991) *Proc. Natl. Acad. Sci. USA* **88**, 3441–3445.
43. Zhu, X., Komiya, H., Chirino, A., Faham, S., Fox, G. M., Arakawa, T., Hsu, B. T. & Rees, D. C. (1991) *Science* **251**, 90–93.